

# Nonlinear absorption of transparent glass ceramics containing sodium niobate nanocrystals

T. R. Oliveira, L. de S. Menezes, and Cid B. de Araújo\*

*Departamento de Física, Universidade Federal de Pernambuco, 50670-901 Recife, Pernambuco, Brazil*

A. A. Lipovskii

*St. Petersburg State Polytechnic University, 29 Polytechnicheskaja, St. Petersburg 195251, Russia*

(Received 6 March 2007; revised manuscript received 24 August 2007; published 30 October 2007)

We report on the nonlinear (NL) optical absorption of glass ceramics containing sodium niobate ( $\text{NaNbO}_3$ ) nanocrystals measured with nanosecond lasers. The NL absorption behavior, associated with samples with different volume fractions occupied by the  $\text{NaNbO}_3$  nanocrystals, was studied using lasers operating at 532, 580, and 610 nm. The intensity response of the samples was understood taking into account the contributions of two-photon absorption (TPA) and excited state absorption (ESA) due to free carriers and electron trapping states. Values for the TPA coefficients and the ESA cross sections were obtained for different samples and excitation wavelengths.

DOI: [10.1103/PhysRevB.76.134207](https://doi.org/10.1103/PhysRevB.76.134207)

PACS number(s): 42.65.-k, 42.62.Fi, 78.20.Ci, 78.67.Bf

## I. INTRODUCTION

Glass ceramics (GCs) are glasses containing nanometer to micrometer sized crystalline inclusions. The optical properties of GCs containing ferroelectric nanocrystals were first studied at the beginning of the 1970s,<sup>1</sup> when it was shown that they were different from those of bulky materials, depending strongly on the nanocrystals' dimensions and the volume fraction of the sample occupied by them, the so-called filling fraction  $f$ . Presently, it is known that to obtain a highly transparent GC, the inclusions must have dimensions much smaller than the wavelength of light. Also important is the refractive index mismatch  $\Delta n$  between the host and the nanocrystals. Large values of  $\Delta n$  contribute to increase the nonlinearity of the GC, but the light scattering cross sections of the grains increase and the light throughput of the samples is reduced. Thus, the selection of materials to be used as host and inclusions is always a challenge.<sup>1-3</sup>

Among the GCs already known, the ones based on alkali metal niobates are of particular interest because they present characteristics appropriate for photonic applications, such as photorefractivity and large second-order nonlinearity when electric poled.<sup>4</sup> However, in general, materials preparation methods lead to poor compositional homogeneity that makes controlling the performance of these materials difficult. For instance, reports on the preparation and optical properties of GC containing sodium niobate nanocrystals (GC-SNN) are in small number because the traditional methods of preparation lead to a poor homogeneity of the samples.

Recently, new methods were developed and samples of good optical quality, containing nanocrystals with size of  $\approx 10$  nm, were obtained.<sup>3</sup> In the last years, the nonlinear (NL) optical properties of GC-SNN and their dependence on the SNN filling fraction were studied. The optical limiting behaviors due to two-photon absorption (TPA) at 532 nm and three-photon absorption at 1064 nm were investigated when exciting the samples with 10 and 15 ns laser pulses, respectively.<sup>5</sup> Z-scan measurements<sup>6</sup> were performed to determine the SNN influence on the NL refractive index  $n_2$  and the TPA coefficient  $\alpha_2$  of the GC-SNN using 70 ps laser pulses at 532 nm.<sup>7,8</sup> In another work, the GC-SNN nonlin-

earity was measured at 800 nm using 100 fs laser pulses and revealed its ultrafast response.<sup>9</sup> Explanations for the dependence of  $n_2$  and  $\alpha_2$  on the excitation wavelength and on the SNN filling fraction were given, and the prospects for using the studied samples in photonic devices were presented in Ref. 8. Optical waveguides were also prepared and characterized for integrated optics applications.<sup>10</sup> More recently, incoherent second harmonic generation was studied via hyper-Rayleigh scattering from GC-SNN allowing the measurement of the hyperpolarizability per nanocrystal.<sup>11</sup>

In the present work, we report on NL absorption measurements for excitation at different wavelengths in the visible range. The experiments, performed with samples having different filling fractions, allowed the determination of the TPA coefficient and the excited state absorption (ESA) cross section for excitation with nanosecond lasers operating at wavelengths in the transparency region of samples.

## II. EXPERIMENTAL DETAILS

The samples studied were based on the following glass composition in mol %:  $35\text{SiO}_2\text{-}31\text{Nb}_2\text{O}_5\text{-}19\text{Na}_2\text{O-}11\text{K}_2\text{O-}2\text{CdO-}2\text{B}_2\text{O}_3$ . The synthesis' procedure was the same as described in Ref. 3: the glass (180 g) was synthesized at 1450 °C with stirring for 2 h in a platinum crucible. In the batch preparation, only chemically pure and high-purity grade reagents were used. The melt was poured onto a preheated brass plate, and the resultant glass was annealed for 2 h at the temperature corresponding to the glass viscosity equal to  $10^{12}$  Pa s ( $\sim 575$  °C). After being prepared, the samples are submitted to a heat treatment at 610 °C to achieve the nucleation of SNN with dimensions of  $\approx 10$  nm, as determined by small-angle x-ray scattering measurements. In this treatment, crucibles with the samples were placed in preliminary heated furnace; according to our estimations, the samples reached the fixed temperature (610 °C) in 3–5 min. Varying the duration of the treatment provided different volume fractions  $f$  of the SNN. After the processing, the samples were removed from the furnace and from the crucible and cooled in air. The growth of nanocrystals occurs at

TABLE I. Parameters of the samples:  $t$  is the heat-treatment time and  $\alpha_0$  is the extinction coefficient. The reflectivity  $R$  was calculated using the measured values of the linear refractive index, considering normal incidence.  $E_g$  is the energy gap of the samples. The large values of  $\alpha_0$  for samples C and D are due to light scattering by clusters of nanocrystals (Ref. 8).

Sample	$t$ (h)	Filling fraction ( $f$ )	$\alpha_0$ (cm <sup>-1</sup> )			$R$	$E_g$ (eV)
			532 nm	580 nm	610 nm		
A	2	0.00	0.41	0.21	0.14	0.092	3.6
B	8	0.03	0.40	0.31	0.21	0.092	3.5
C	16	0.08	1.15	0.70	0.54	0.095	3.3
D	33	0.19	1.99	1.28	1.02	0.100	3.2
E	69	0.36	0.46	0.28	0.22	0.106	3.2
G	141	0.37	0.17	0.11	0.07	0.107	3.2
H	206	0.37	0.17	0.11	0.07	0.108	3.2

temperatures above  $\sim 580$  °C, and the formation of the SNN practically coincides with the thermal treatment time. Samples with different values of  $f$  as shown in Table I were obtained. The  $f$  values were found using the known density of sodium niobate crystal and densitometry data of the initial glasses, formed glass ceramics, and especially melted set of glasses with deficit of both sodium and niobium oxides. This allowed the estimation of the density of the glass part of glass ceramics after the growth of SNN.<sup>3</sup> The accuracy of the filling fraction estimation is the same as the accuracy of density measurements, i.e.,  $\sim 0.5\%$  assuming that the volume fraction of SNN-glass interfacial layer is low in comparison with the volume of the nanocrystal.

The NL measurements were performed using the second harmonic of a  $Q$ -switched Nd:YAG (yttrium aluminum garnet) laser (532 nm, 7 ns, and 5 Hz) and dye lasers, pumped by the 532 nm beam, emitting linearly polarized light in the range 570–630 nm. To control the optical power incident on the sample, the laser beam was made to pass through a half-wave plate combined with a polarizer. Then, a lens (focal length of 10 cm) focused the beam on the sample, which was positioned at the place of smaller beam-waist size, as determined using the knife-edge technique.<sup>12</sup> Two large area photodiodes were calibrated to measure independently the incident power on the sample and the transmitted intensity. Care was taken to collect all transmitted light to avoid errors in the NL measurements. The electronic signal was recorded using a digital oscilloscope, a boxcar, and a computer.

### III. RESULTS AND DISCUSSION

The optical absorption spectra of the samples were shown in the previous publications.<sup>7–9</sup> They exhibit a large transparency window from the near infrared to the visible, and the onset of absorption lies in the blue-green region. The optical gap for each sample is given in Table I.

The results obtained in the NL measurements are shown in Figs. 1(a)–1(c), corresponding to excitation wavelengths of 532 nm (for samples B, C, D, and G) and 580 and 610 nm

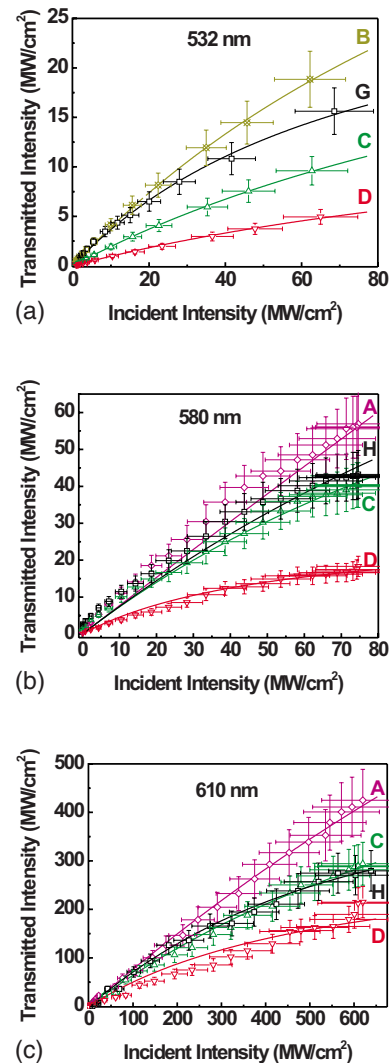


FIG. 1. (Color online) Transmitted intensity as a function of the incident intensity for glass-ceramic samples containing sodium niobate nanocrystals with different filling fractions. Excitation wavelengths: (a) 532 nm, (b) 580 nm, and (c) 610 nm. The symbols correspond to experimental data. The solid lines represent a theoretical fit of Eq. (3) to the data.

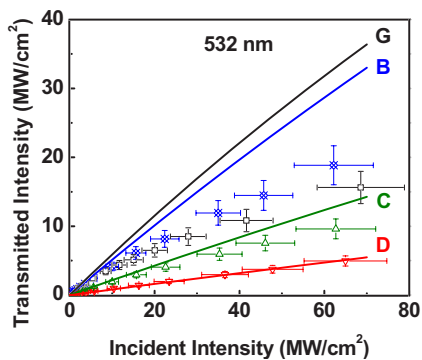


FIG. 2. (Color online) Comparison between the results obtained in the present experiments with the theoretical curves corresponding to Eq. (3) assuming  $\alpha_2$  values obtained with 80-ps-long excitation pulses (Ref. 8).

(for samples A, C, D, and H), respectively. The points illustrate the behavior of the transmitted intensity as a function of the laser intensity with an estimated error of 15% in the intensity measurements. The behavior of the other samples is analogous. The NL absorption increases for increasing values of  $f$ , but the NL behavior is less pronounced for wavelengths that are more detuned from the samples' band gap. Because 610 nm corresponds to photons with larger detuning with respect to the samples' band gap, the results of Fig. 1(c) were obtained with larger laser intensities than Figs. 1(a) and 1(b). For a given excitation wavelength, the magnitude of the NL absorption is larger for larger SNN filling fractions. The solid lines in the figures are obtained using a model described below.

The results could not be fitted considering only the TPA process. For increasing laser intensities, the data deviate from the usual quadratic dependence observed when pure TPA is present. This is demonstrated in Fig. 2, which shows the theoretical curves corresponding to  $\alpha_2$  values obtained with 80-ps-long excitation pulses<sup>8</sup> assuming that TPA is the dominant process. The points are the results obtained in the present experiments. It is clear that an extra NL absorption contribution related to the nanocrystals is present. When exciting the samples with nanosecond pulses, the NL absorp-

tion can be influenced by TPA as well as by the free carriers generated in the TPA process and electrons trapped in localized states due to defects in the SNN interfaces. The contribution of both types of excited states was previously studied in semiconductors<sup>13</sup> and in glasses doped with semiconductor nanocrystals.<sup>14–19</sup> In GC with alkali metal niobate nanocrystals, it has never been reported. For smaller pulse widths, as in Refs. 8 and 9, the contribution of the bound electrons was dominant.

The ESA contribution depends on the laser fluence as well as on the laser intensity, whereas the bound electronic nonlinearity depends only on the intensity. The magnitude of the TPA coefficient  $\alpha_2$  and the ESA cross section  $\sigma_{ESA}$  were determined for each sample and for each excitation wavelength by analyzing the light attenuation through the samples that is described by

$$\frac{dI(z)}{dz} = -\alpha_0 I(z) - \alpha_2 I^2(z) - \sigma_{ESA} N I(z), \quad (1)$$

where  $I(z)$  is the light intensity along the propagation direction  $z$  and  $\alpha_0$  is the extinction coefficient. The term  $-\alpha_2 I^2(z)$  is due to the TPA process. The last term represents the ESA contribution, with  $N$  being the photogenerated carrier density governed by the equation  $dN/dt = \alpha_0 I(z)/\hbar\omega + [\alpha_2 I(z)/2\hbar\omega]I(z)$ . For a Gaussian laser pulse represented by the expression  $I(z, t) = I(z)\exp(-t^2/\tau^2)$ , where  $\tau$  is the laser pulse duration, one obtains  $N = (\alpha_0 \tau \sqrt{\pi}/\hbar\omega)I(z) + \sqrt{\pi/2}(\alpha_2 \tau/2\hbar\omega)I^2(z)$ . When inserted in Eq. (1), this leads to

$$\frac{dI(z)}{dz} = -[\alpha_0 + (\alpha_2 + \delta)I(z) + \gamma I^2(z)]I(z), \quad (2)$$

where  $\delta = \sqrt{\pi}(\alpha_0 \tau \sigma_{ESA}/\hbar\omega)$  and  $\gamma = \sqrt{\pi/2}(\alpha_2 \tau \sigma_{ESA}/2\hbar\omega)$ . Thus, an effective intensity dependent NL absorption coefficient can be defined as  $\alpha_2^{eff}(I) = (\alpha_2 + \delta) + \gamma I$ .

As shown in the Appendix, integrating Eq. (2) and taking into account the sample reflectivity  $R$  in each of its faces, one obtains a relation between the intensity transmitted through the sample and the incident intensity given by

$$I_L = \frac{(1-R)^2 I_0 e^{-\alpha_0 L} [\alpha_0 + (\alpha_2 + \delta)I_L + \gamma I_L^2]^{+0.5} [\alpha_0 + (\alpha_2 + \delta)I_0(1-R) + \gamma I_0^2(1-R)^2]^{-0.5}}{\left( \frac{\sqrt{\Delta} + (\alpha_2 + \delta) + 2\gamma I_L \sqrt{\Delta} - (\alpha_2 + \delta) - 2\gamma I_0(1-R)}{\sqrt{\Delta} - (\alpha_2 + \delta) - 2\gamma I_L \sqrt{\Delta} + (\alpha_2 + \delta) + 2\gamma I_0(1-R)} \right)^{(\alpha_2 + \delta)/2\sqrt{\Delta}}}, \quad (3)$$

where  $I_0 = I(z=0)$  and  $\Delta = (\alpha_2 + \delta)^2 - 4\alpha_0\gamma$ . We notice that Eq. (2) was considered to describe the NL absorption in chalcogenide glasses,<sup>20</sup> where a quasianalytical solution was given. However, the result presented in Eq. (3) is more general, being valid for arbitrary values of  $I_0$  and having the result presented in Ref. 20 as a limiting case.

Equation (3) has two independent parameters,  $\alpha_2$  and  $\sigma_{ESA}$ , that can be found using a NL curve fitting procedure to obtain the best agreement with the experimental data. However, the values of  $\alpha_2$  at 532 nm, shown in Table II, were previously measured using the Z-scan technique in the picosecond regime.<sup>8</sup> Considering that in the picosecond experi-

TABLE II. Nonlinear parameters obtained by fitting Eq. (3) to the experimental data (estimated error: 15%). The values for  $\alpha_2$  at 532 nm were previously reported for 80 ps pulses Ref. 8.

Sample	$\alpha_2$ (cm/GW)			$\sigma_{ESA}$ ( $\times 10^{-19}$ cm $^2$ )		
	532 nm	580 nm	610 nm	532 nm	580 nm	610 nm
A	0.54	0.21	0.14	—	0.33	0.32
B	0.55	—	—	9.80	—	—
C	0.60	0.40	0.17	2.98	2.37	0.85
D	0.70	0.58	0.20	0.27	13.8	1.35
E	0.88	0.84	0.29	—	2.19	1.00
G	0.90	—	—	28.1	—	—
H	0.90	0.86	0.30	—	4.93	1.02

ments there was no contribution of ESA, those values were used in the analysis of the present experiment to obtain the value for  $\sigma_{ESA}$  at 532 nm. Then, the value of  $\sigma_{ESA}$  obtained for 532 nm was used as the starting value in the fitting procedure to determine the NL parameters at 580 and 610 nm. The solid lines in Figs. 1(a)–1(c) represent the solution of Eq. (3) with the best-fit values obtained using the MATHCAD® software. The NL parameters obtained are summarized in Table II. We note that  $\alpha_2$  for each wavelength grows for increasing  $f$  values. As shown in Ref. 8, the behavior of  $\alpha_2$  with  $f$  can be predicted using the generalized NL Maxwell-Garnet model.<sup>21</sup> According to this model, the samples are considered as containing spherical inclusions dispersed in a uniform host with an effective dielectric function given by

$$\varepsilon_{eff} = \varepsilon_h \left[ 1 + \frac{3\beta f}{1 - \beta f} \right], \quad (4)$$

where  $\beta$  is given by

$$\beta = \frac{\varepsilon_i - \varepsilon_h}{\varepsilon_i + 2\varepsilon_h}, \quad (5)$$

with  $\varepsilon_i$  and  $\varepsilon_h$  being the linear dielectric functions of the NaNbO<sub>3</sub> nanocrystals and the host medium, respectively. In the NL regime, the Maxwell-Garnet model predicts that the effective third-order susceptibility is given by

$$\chi_{eff}^{(3)} = \frac{\chi_h^{(3)} + f\{C_i - \chi_h^{(3)}[1 - 4(2\beta^4 + 2\beta^3 + 9\beta^2)/5]\}}{(1 - \beta f)^4}, \quad (6)$$

with

$$C_i = \frac{81\chi_i^{(3)}}{[2 + (\varepsilon_i/\varepsilon_h)]^4}, \quad (7)$$

where  $\text{Im } \varepsilon_i$  and  $\text{Im } \varepsilon_h$  were neglected.  $\chi_i^{(3)}$  and  $\chi_h^{(3)}$  are the NL susceptibilities of the inclusions and host medium, respectively. The TPA coefficient is determined by  $\alpha_2 = (3\omega/2cn_0) \text{Im } \chi_{eff}^{(3)}$ .

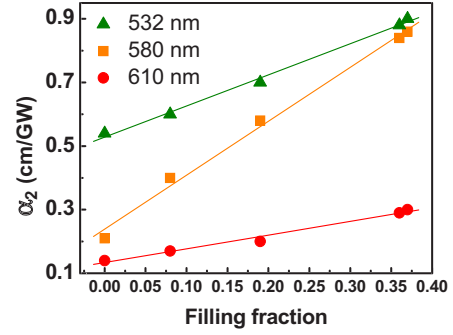


FIG. 3. (Color online) Two-photon absorption coefficients  $\alpha_2$  (given in Table II) for different excitation wavelengths: 532 nm (triangles), 580 nm (squares), and 610 nm (circles). The results follow a linear dependence with  $f$ .

Figure 3 shows that the  $\alpha_2$  values, given in Table II, are linearly dependent on  $f$ , as predicted by the Maxwell-Garnet model.<sup>8</sup> The larger derivative of  $\alpha_2$  in relation to  $f$  for excitation at 580 nm indicates a possible two-photon resonance with states due to defects. We recall that the presence of excited states due to defects localized on the nanocrystals and/or their boundaries, in the 4 eV region, was recently reported for NaNbO<sub>3</sub> films.<sup>22</sup>

The dependence of  $\sigma_{ESA}$  on  $f$  and the light wavelength cannot be predicted *a priori* because the concentration of surface defects and the number density of electrons trapped in the defects are unknown. Furthermore, accidental resonances of the light frequency with excited states may occur. This is clearly illustrated in Table II, which shows a large dispersion in the  $\sigma_{ESA}$  values ( $0.27 \leq \sigma_{ESA} \leq 28.1$ ).

In summary, in this work, the dispersion of the NL absorption in glass ceramics containing sodium niobate nanocrystals (with different filling fractions up to  $\approx 40\%$ ) was studied in the nanosecond regime. The NL absorption process was investigated at the excitation wavelengths of 532, 580, and 610 nm. The results show that the nanocrystals play a prior role in the magnitude of  $\alpha_2$  and, consequently, in the behavior of the sample face to TPA. A solution for the laser beam propagation equation, considering the contributions of TPA and ESA, was obtained. Only by considering the ESA term was it possible to get good fits to the experimental results, showing the importance of this process when exciting the samples with nanosecond pulses.

#### ACKNOWLEDGMENTS

We acknowledge the financial support from the Brazilian agencies Conselho Nacional de Desenvolvimento Científico e Tecnológico (CNPq), Fundação de Amparo à Ciência e Tecnologia de Pernambuco (FACEPE), and Coordenação de Aperfeiçoamento de Pessoal de Ensino Superior (CAPES). We also thank B. J. P. da Silva for cutting and polishing the samples.

#### APPENDIX

In the presence of significant TPA in a material, excited state absorption (ESA) can ensue from the two-photon pumped state. Thus, the attenuation equation for a beam

propagating through a material is given by Eq. (2) that includes TPA and ESA contributions. In order to integrate Eq. (2), let us define some parameters:

$$P = a + bx + cx^2,$$

$$a = \alpha_0, \quad b = \alpha_2 + \delta, \quad c = \gamma, \quad x = I. \quad (A1)$$

The introduction of Eqs. (A1) in Eq. (2) for  $a, b, c > 0$  and for a sample of length  $L$  leads to

$$-L = \int_{I_0}^{I_L} \frac{dx}{xP} = \left[ \frac{1}{2a} \ln\left(\frac{x^2}{P}\right) + \frac{b}{a\sqrt{\Delta}} \operatorname{arctgh}\left(\frac{b+2cx}{\sqrt{\Delta}}\right) \right]_{I_0}^{I_L}, \quad (A2)$$

with  $\Delta$  defined as in Sec. III and  $I_L = I(z=L)$ . The solution for this integral is given in Ref. 23. After algebraic manipulation of Eq. (A2), we obtain

$$I_L = \frac{I_0 e^{-\alpha_0 L} [\alpha_0 + (\alpha_2 + \delta)I_L + \gamma I_L^2]^{+0.5} [\alpha_0 + (\alpha_2 + \delta)I_0 + \gamma I_0^2]^{-0.5}}{\left( \frac{\sqrt{\Delta} + (\alpha_2 + \delta) + 2\gamma I_L}{\sqrt{\Delta} - (\alpha_2 + \delta) - 2\gamma I_0} \right)^{(\alpha_2 + \delta)/2\sqrt{\Delta}}}, \quad (A3)$$

which relates  $I(z=L)$  with the incident intensity  $I_0$ .

\*Corresponding author: cid@df.ufpe.br

<sup>1</sup>N. F. Borrelli and M. M. Layton, *J. Non-Cryst. Solids* **6**, 197 (1971).

<sup>2</sup>P. A. Tick, N. F. Borrelli, and I. M. Reaney, *Opt. Mater. (Amsterdam, Neth.)* **15**, 81 (2000).

<sup>3</sup>A. A. Zhilin, G. T. Petrovsky, V. V. Golubkov, A. A. Lipovskii, D. K. Tagantsev, and B. V. Tatarintsev, *J. Non-Cryst. Solids* **345&346**, 182 (2004); A. A. Lipovskii, D. K. Tagantsev, B. V. Tatarintsev, and A. A. Vetrov, *ibid.* **318**, 268 (2003).

<sup>4</sup>A. Malakho, E. Fargin, M. Lahaye, B. Lazoryak, V. Morozov, G. van Tendeloo, V. Rodriguez, and F. Adamietz, *J. Appl. Phys.* **100**, 063103 (2006).

<sup>5</sup>G. S. Maciel, N. Rakov, C. B. de Araújo, A. A. Lipovskii, and D. K. Tagantsev, *Appl. Phys. Lett.* **79**, 584 (2001).

<sup>6</sup>M. Sheik-Bahae, A. A. Said, T. H. Wei, D. J. Hagan, and E. W. van Stryland, *IEEE J. Quantum Electron.* **26**, 760 (1990).

<sup>7</sup>G. S. Maciel, C. B. de Araújo, A. A. Lipovskii, and D. K. Tagantsev, *Opt. Commun.* **203**, 441 (2002).

<sup>8</sup>E. L. Falcão-Filho, C. A. C. Bosco, G. S. Maciel, L. H. Acioli, C. B. de Araújo, A. A. Lipovskii, and D. K. Tagantsev, *Phys. Rev. B* **69**, 134204 (2004).

<sup>9</sup>C. A. C. Bosco, E. L. Falcão-Filho, G. S. Maciel, L. H. Acioli, C. B. de Araújo, A. A. Lipovskii, and D. K. Tagantsev, *J. Appl. Phys.* **94**, 6223 (2003).

<sup>10</sup>A. A. Lipovskii, D. V. Svistunov, D. K. Tagantsev, B. V. Tatarintsev, and P. G. Kazansky, *Mater. Lett.* **58**, 1231 (2004).

<sup>11</sup>E. Valdez, C. B. de Araújo, and A. A. Lipovskii, *Appl. Phys. Lett.* **89**, 031901 (2006).

<sup>12</sup>A. Siegman, M. W. Sasnett, and T. F. Johnston, Jr., *IEEE J. Quantum Electron.* **27**, 1098 (1991).

<sup>13</sup>A. A. Said, M. Sheik-Bahae, D. J. Hagan, T. H. Wei, J. Wang, J. Young, and E. W. van Stryland, *J. Opt. Soc. Am. B* **9**, 405 (1992).

<sup>14</sup>H. Ma, A. S. L. Gomes, and C. B. de Araújo, *J. Opt. Soc. Am. B* **9**, 2230 (1992).

<sup>15</sup>H. Ma and C. B. de Araújo, *Opt. Commun.* **110**, 627 (1994).

<sup>16</sup>G. Boudebs and C. B. de Araújo, *Appl. Phys. Lett.* **85**, 3740 (2004).

<sup>17</sup>M. Yamane and Y. Asahara, *Glasses for Photonics* (Cambridge University Press, Cambridge, UK, 2000), and references therein.

<sup>18</sup>L. Razzari, A. Gnoli, M. Righini, A. Dâna, and A. Aydinli, *Appl. Phys. Lett.* **88**, 181901 (2006).

<sup>19</sup>L. A. Padilha, J. Fu, D. J. Hagan, E. W. Van Stryland, C. L. Cesar, L. C. Barbosa, C. H. B. Cruz, D. Buso, and A. Martucci, *Phys. Rev. B* **75**, 075325 (2007).

<sup>20</sup>S. Cherukulappurath, J. L. Godet, and G. Boudebs, *J. Nonlinear Opt. Phys. Mater.* **14**, 49 (2005).

<sup>21</sup>J. E. Sipe and R. W. Boyd, *Phys. Rev. A* **46**, 1614 (1992).

<sup>22</sup>I. Aulika, J. Petzelt, J. Pokorný, A. Deyneka, V. Zauls, and K. Kundzins, *Rev. Adv. Mater. Sci.* **15**, 158 (2007).

<sup>23</sup>I. S. Gradshteyn and I. M. Ryzhik, *Table of Integrals Series and Products* (Academic, New York, 1965).